

# Prediction of Ductile Fracture of High-Rate Loaded Steel Structures

G. Pape<sup>1</sup>, M. Janssen<sup>1</sup> and A. Bakker<sup>1</sup>

<sup>1</sup> Delft University of Technology, Laboratory of Materials Science, Delft, The Netherlands

**ABSTRACT:** *The prediction of damage subsequent to internal explosions has been a subject of interest for many years now. In order to be able to analyse the deformation and failure behaviour by numerical methods, experiments have been performed on steel plate material to derive the deformation and fracture behaviour. These experiments are performed for varying deformation rates to account for the influence of the strain rate in actual high-rate loaded structures. The flow stress of the material is examined as a function of plastic strain and strain rate. High-speed photography is applied to investigate the necking behaviour at high strain rates. The fracture behaviour of the plate material is examined by testing a number of notched specimens with different notch radii at various strain rates. The influence of the notch radius, and therefore the hydrostatic stress, becomes evident from these experiments. Failure strains decrease strongly with decreasing notch radius; however the strain rate has negligible influence on the fracture strain. Modelling these experiments using the strain-rate-dependent flow stress derived from the tensile tests results in fairly good agreement with the experimental results. The ductile damage is accounted for using the Rice and Tracey fracture model. Predictions of failure cannot be made so accurate, as the failure mechanism is not described very well. Investigations on the micromechanical behaviour of fracture must reveal the shortcomings of the failure analysis.*

## INTRODUCTION

The present work aims at an improvement of modelling techniques to assess the failure behaviour of high-rate loaded structures. High-rate loading of structures involving large plastic deformations and fracture arise mainly from accidental occasions or deliberate destruction attempts. For example explosions in war due to enemy attack causes large damage to ships. The prediction of damage caused by internal explosions has been a subject of interest for many years now. Large-scale experiments on real ship structures as well as on structural components such as bulkheads have been carried out in the past. These experiments reveal the failure behaviour during high rate loading due to internal explosions. The bulkheads tend to rupture near the

welded edges. Microscopic analysis of bulkhead material close to the fractured zone reveals that the rupture occurs outside the weld and heat affected zone. Therefore it has been decided to investigate the plate material of the bulkhead. Investigation of the heat-affected-zone material is a secondary point of interest.

## **APPROACH OF THE PROBLEM**

A failure prediction of high rate loaded structures such as bulkheads inside a ship during internal explosion loading can be performed using the Finite Element Method. This requires the flow stress of the material to be known as a function of the plastic strain and strain rate. The flow stress has to be known up to large strains as large deformations develop locally in the structure prior to fracture initiation. The flow stress is determined by experiments on the plate material.

The failure behaviour of the material is investigated in order to compare numerical predictions of failure with actual material behaviour. The influence of strain rate is considered as well. A failure model is implemented in a Finite Element program. The strain-rate-dependent flow stress is used for the calculations. In this way the influence of the strain rate on the failure predictions is accounted for.

If a good comparison can be made between numerical failure predictions and experiments, the model can be applied to larger specimens. These larger specimens contain welds and represent a small part of an actual structure. When the model predicts the failure behaviour accurately for the larger specimens, it can be applied to complete structures. A comparison of numerical failure predictions can be made with full scale experiments on explosion loaded bulkheads.

When the weld region of the bulkheads or large specimens appears to be important as well, these materials will be investigated in a similar way as the plate material. Some tensile tests on heat affected zone material have been performed already.

## **EXPERIMENTAL RESULTS**

The experimental results obtained as described in the previous section will be presented here. First, the influence of the strain rate on the stress-strain curve is investigated. Secondly, the influence of the strain rate and the

hydrostatic stress is investigated. Attention is given to the influence of the plate rolling direction as well.

### ***Dependence of Flow Stress on Plastic Strain and Strain Rate***

To derive the deformation behaviour of the plate material as a function of the plastic strain and strain rate, tensile tests have been performed on smooth round (5mm diameter) specimen. For low strain rates ( $10^{-5} - 10^{-1} \text{ s}^{-1}$ ) the uniaxial deformation has been measured using a strain gauge extensometer. At high strain rates, a high-speed camera has been used to capture images of the deforming specimen [1]. The distance in the specimen's axial direction between two markers is measured from scanned high-speed photographs. These measurements are used to derive the axial strain at high strain rates up to  $200 \text{ s}^{-1}$ . When necking occurs, the true strain is measured from the diameter reduction at the neck. At low strain rate, the diameter reduction is taken from digital images captured during the experiment. At high strain rates the images of the high-speed camera are used.

At low strain rates the load measurement is performed using a standard strain-gauge loadcell. For the high strain-rate experiments a piezo-electric load transducer is applied [2]. The load signal is smoothed to eliminate the oscillations due to dynamic effects in the loadcell and the system. Using the load signal and the elongation and diameter reduction measurements, the true stress-strain curves are calculated for several strain rates varying from  $10^{-5} \text{ s}^{-1}$  to  $200 \text{ s}^{-1}$ . These strain rates are calculated from the engineering strain. Actual strain rates in the neck increase by a factor of 30 during necking of the specimen, since the tensile velocity is kept constant. When necking occurs, the stress state at the neck is not uniaxial anymore. Also a hydrostatic stress exists at the neck. The true stress is corrected to account for the effect of the hydrostatic stress [3, 4].

A curve-fit is made on the experimental data. The curve-fit gives a relation between the flow stress (after correction), the plastic strain and the plastic strain rate. This curve-fit is used in Finite Element calculations.

### ***Fracture Behaviour***

In order to investigate the influence of the hydrostatic stress on the fracture behaviour of the plate material, tensile specimens have been tested with different notch radii, see Figure 1. The notch radius influences the hydrostatic stress. The strain rate is varied in order to analyse the influence of the strain rate on the failure behaviour. For all strain rates, varying from  $10^{-5}$  to  $10^3 \text{ s}^{-1}$ , the failure mechanism remains ductile. The failure strains are

shown in Figure 2. The open markers refer to specimens loaded perpendicular to the rolling direction; solid markers are in the rolling direction.

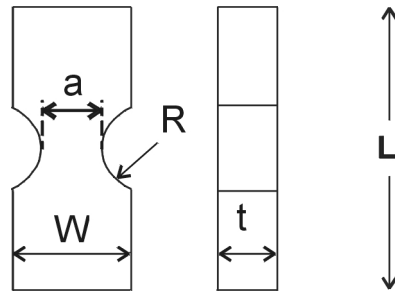


**Figure 1:** Notched specimen [mm],  $W = 10$ ,  $a = 5$ ,  $t = 5$ ,  $L = 37.5$ , Radius  $R$  has been chosen at 5, 1 and 0.45.

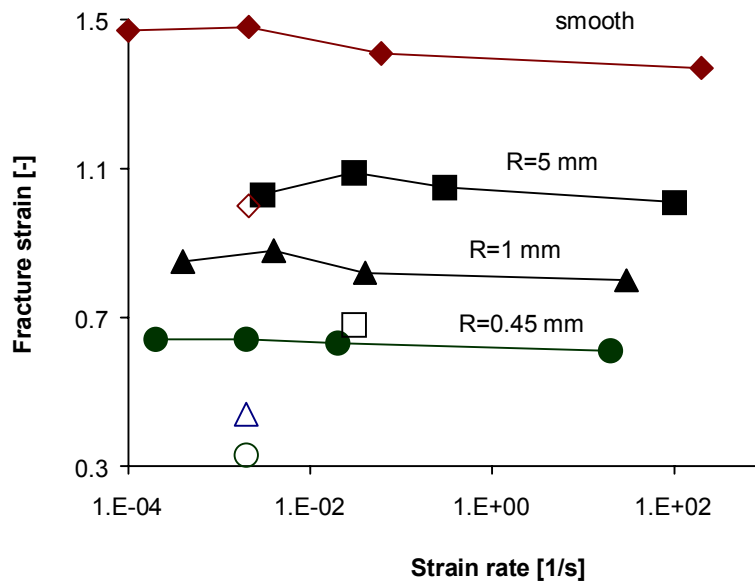


**Figure 2:** Fracture strains from area reduction for smooth and notched specimens at several strain rates. Strain rates are average values related to area reductions. Fracture strain standard deviations vary from 0.01 to 0.05.

## NUMERICAL MODELLING

Finite Element simulations of the experiments are performed in order to compare the numerical predictions of ductile failure with the experimental results. To verify the deformation behaviour predictions, the curve-fit of the experimental flow stress as a function of the plastic strain and plastic strain rate is implemented in the Finite Element program. The failure behaviour is predicted using a local failure criterion.

### *Deformation Behaviour*

Tensile tests on smooth round specimens as well as on notched flat specimens have been numerically simulated using the experimentally determined flow stress. The graph in Figure 3 shows the calculated load – elongation curves for a smooth specimen at three different strain rates.

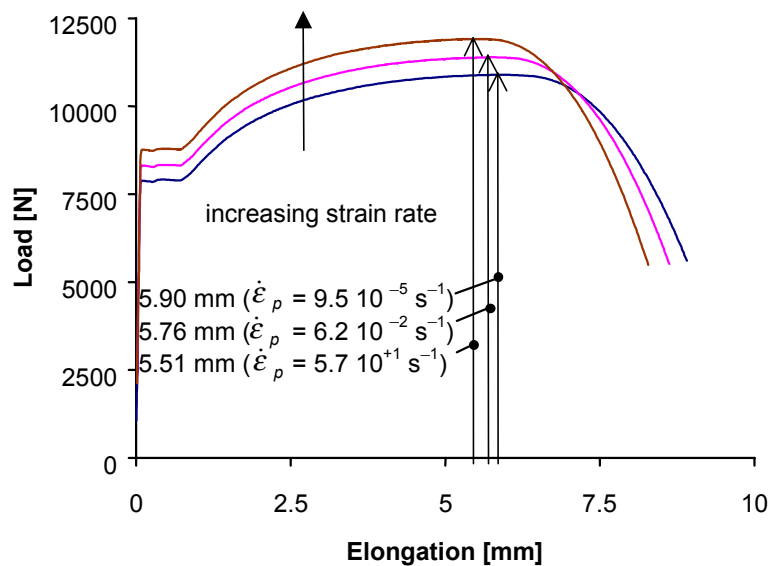


**Figure 3:** Results from finite element calculations: load - displacement curves up to the experimentally determined failure strains at different strain rates. Initial specimen gauge length  $L_0$  is 35 mm.

A larger strain rate causes the load to increase and the strain at which necking starts to slightly decrease. The load increase is in agreement with the experimental results (not plotted in the graph); the decrease of strain where necking starts is hard to detect from the experimental results.

Comparison of true stress – strain curves for different strain rates shows good agreement before necking starts. During necking at high strain rates the true stress is overestimated by no more than 7%, this error decreases at lower strain rates.

The comparison between load – elongation curves for tensile test simulations and experiments on notched specimen give a fairly good agreement for all strain rates ( $\approx 10^{-4} \text{ s}^{-1} - 10^2 \text{ s}^{-1}$ ), i.e. almost within the accuracy of the experiments. The load tends to be underestimated with a few percents.

### ***Failure Predictions***

To predict the ductile failure behaviour by a numerical model, the Rice and Tracey [5] model is applied, i.e.

$$\ln\left(\frac{r}{r_0}\right) = 0.283 \cdot \int_{\varepsilon_p} \exp(A_{RT} \cdot \sigma_h / \sigma_e) \, d\varepsilon_p \quad (1)$$

In Eq. 1  $r$  is the radius of a void in the material growing during plastic deformation. The initial void radius is  $r_0$  and  $\varepsilon_p$  denotes the equivalent plastic strain. The void growth rate void depends exponentially on the ratio of the hydrostatic stress  $\sigma_h$  and the equivalent Von Mises stress  $\sigma_e$ . In the original model by Rice and Tracey, the constant  $A_{RT}$  has the value 1.5.

In the numerical simulations performed for smooth and notched specimens the evolution of a fictitious void is calculated for each material point. The calculations are performed up to the point where the area reduction at the minimum cross section (at the notch or neck) equals the experimental value measured from the fractured specimen. The graph in Figure 4 shows the development of the ratio  $r/r_0$  for all specimens at low strain rate (approximately  $10^{-3} \text{ s}^{-1}$ ). The true strain is derived from area reduction at the notch or neck. The locations where the void radius is evaluated is chosen at the point of maximum damage at the moment that the area reduction in the calculation equals the experimental area reduction at fracture. The position for the smooth geometry and notch with radius of 5 mm is at the centre of the specimen, while for notch radii of 1 mm and 0.45 mm this position is at the centre of the notch tip. From the graph it can be seen that the relative void radius at fracture has no unique value for the different specimen geometries. The ratios vary from 2.3 to 3.8.

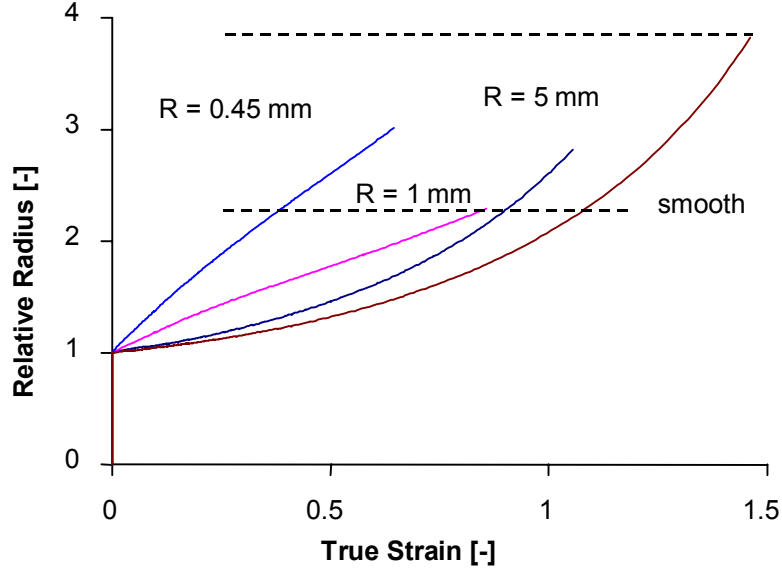


**Figure 4:** Damage predictions for low strain rates according to Rice and Tracey ( $A_{RT} = 1.5$ ). Dotted lines represent the range of numerical prediction of the relative void radius.

The influence of the strain rate is also investigated by numerical simulations. For this the relative void radius at fracture is assumed not to depend on strain rate. It is found that for every increase of strain rate by a factor of 10 the failure strain reduces about 0.02 for the smooth specimen, 0.015 for the  $R = 5$  mm specimen and about 0.01 for both the  $R = 1$  and 0.45 mm geometries. These results are in agreement with experimental values taking into account the experimental scatter.

In order to improve the results a mesh was chosen with equally-sized elements in front of the notch tip. The average value of the relative void radius is used for failure predictions. The physical interpretation is that the damage averaged over a certain material volume is the determining factor. The critical value for  $r/r_0$  for the notched geometries is  $2.5 \pm 0.35$ . Prediction of failure at low strain rates for  $r/r_0 = 2.5$  gives the results shown in Table 1.

TABLE 1: Comparison of numerical predictions with experimental values for strain from area reduction at failure initiation.

	smooth	$R = 5$ mm	$R = 1$ mm	$R = 0.45$ mm
Experiment	1.47	0.9 – 1.03	0.75 – 0.85	0.55 – 0.64
Prediction	1.2	0.97	0.87	0.44

## CONCLUSIONS & RECOMMENDATIONS

The strain rate dependent flow stress formulation derived from the experimental results can be applied for finite element calculations with reasonable accuracy.

When predicting using the Rice and Tracey model the effect of the hydrostatic stress cannot be accurately taken into account. The influence of the strain rate on the fracture strain is well accounted for when a strain rate dependent flow stress is applied. The failure predictions fall within the experimental scatter.

Applying a constant element length and averaging the void radius over each element yield failure predictions with moderate accuracy. Further investigation of the model is a prerequisite for improvement. The actual void growth has to be analysed and compared with calculations.

The Rice and Tracey model can be investigated for failure predictions of heat affected zone material, see the Introduction.

## ACKNOWLEDGEMENT

This research was funded by the Technology Foundation STW, the TNO Prins Maurits Laboratory and the Delft University of Technology.



## REFERENCES

1. Pape, G., Bakker, A. (1999). In: *Proc. Int. Workshop on Video-Controlled Materials Testing and In-situ Microstructural Characterization*, pp. 165 – 168, Nancy, France.
2. Pape, G., Bakker, A. (1998). In: *Proc. ECF 12 – Fracture from Defects*, Vol. 3, pp. 1343 – 1348, Brown, M.W., de los Rios, E.R., Miller, K.J. (Eds.), Emas Publishing, Sheffield.
3. Bakker, A. (1990). In: *Proceedings of the 5<sup>th</sup> International Conference on Numerical Methods in Fracture Mechanics*, pp. 433 – 449, Luxmoore, A.R., Owen, D.R.J. (Eds.), Pineridge, 1990, Freiburg.
4. Bridgman, P.W. (1952). *Studies in Large Plastic Flow and Fracture*. McGraw-Hill Book Company, New York.
5. Rice, J.R., Tracey, D.M. (1969). *Journal of the Mechanics and Physics of Solids* **17**, 201.